Structural and optical properties of (TlInS$_2$)$_{0.75}$(TlInSe$_2$)$_{0.25}$ thin films deposited by thermal evaporation

I. Guler[1,*] , M. Isik[2], and N. Gasanly[3]

[1] Physics, Inter-Curricular Courses Department, Çankaya University, 06530 Ankara, Turkey
[2] Department of Electrical and Electronics Engineering, Atilim University, 06836 Ankara, Turkey
[3] Department of Physics, Middle East Technical University, 06800 Ankara, Turkey

ABSTRACT

Layered semiconductor materials have become a serious research topic in recent years, thanks to their effective optical properties. In this article, the thin-film structure of Tl$_2$In$_2$S$_3$Se [(TlInS$_2$)$_{0.75}$(TlInSe$_2$)$_{0.25}$] material with layered structure was grown by thermal evaporation method. The structural, morphological, and optical properties of the deposited thin films were examined. X-ray diffraction (XRD), energy-dispersive spectroscopy (EDS) and atomic force microscopy (AFM) techniques were used to get information about structural and morphological properties of the thin films. XRD pattern presented well-defined peaks associated with monoclinic crystalline structure. The crystallite size, dislocation density, and lattice strain of the films were also obtained from the analyses of XRD pattern. EDS analysis showed that atomic compositional ratios of the Tl, In, S, and Se elements are consistent with chemical formula of Tl$_2$In$_2$S$_3$Se. The optical characterization of thin film was performed using transmission and Raman spectroscopy techniques. Raman spectrum offered information about the vibrational modes of the thin film. The analyses of the transmission spectrum presented the indirect and direct band gap energies of the Tl$_2$In$_2$S$_3$Se thin film as 2.23 and 2.52 eV, respectively. The further analyses on the absorption coefficient resulted in Urbach energy of 0.58 eV.

1 Introduction

Materials with layered structures have become an important research topic in recent years, thanks to their ability to be made two-dimensional (2D). Especially, the optical properties of two-dimensional structures have made these materials the most effective in technological applications. High mobility, high conductivity, and efficient mechanical properties have also made these materials attractive for optoelectronic applications. Ternary semiconductor materials with Tl-III-VI$_2$ structure (III = Ga and In

and VI = S) are layered compounds and can be converted into 2D by mechanical methods. $TlInS_2$ has an important position in this group and has effective optical properties that can be used in optoelectronic applications. As a result of the replacement of the S atom with Se in the $TlInS_2$ compound, $TlInS_{2-2x}Se_{2x}$ quaternary semiconductor materials are formed. As a result of the replacement of the S atom with the Se atom, the structural and optical properties of the $TlInS_2$ material can be changed in desired purposes. For example, while the indirect band gap energy of the $TlInS_2$ crystal is 2.26 eV, the direct band gap of the $TlInSe_2$ crystal, which is formed by completely replacing the S atom with the Se atom, decreases to 1.1 eV [1, 2]. For this reason, the characterizations of the structures formed by the displacement of atoms have become an important subject of research.

$Tl_2In_2S_3Se$ compound belongs to the group of semiconductors with layered structure and is the structural analog of $TlInS_2$, in which one quarter of sulfur atoms are replaced by selenium atoms (x = 0.25 in $TlInS_{2-2x}Se_{2x}$). The crystal lattice of the quaternary compound consists of alternating 2D layers arranged parallel to the (001) plane. Each successive layer is rotated by a 90° angle with respect to previous one. Interlayer strong bonding is formed between Tl and S(Se) atoms, while the bonding between In and S(Se) atoms is of weak intralayer type. The analyses of transmission and reflection spectra of the $Tl_2In_2S_3Se$ crystal resulted in indirect and direct band gap energies of 2.16 and 2.42 eV, respectively [3]. Density-functional theory studies [4], Raman [5], thermoluminescence [6], ellipsometry [7], and thermally stimulated current [8] measurements were carried out to get information about structural, optical, and electrical properties of bulk $Tl_2In_2S_3Se$ single crystal. As it is known, the optical properties of the materials can be changed by changing their thicknesses. The thickness of the bulk crystalline materials that are thick enough is reduced and the optical properties of the thin film and/or 2D materials can vary significantly. In addition, by converting the crystal materials in bulk form into thin-film structure, their use in technological applications becomes more effective. Although $Tl_2In_2S_3Se$ single crystals have been investigated in detail in the literature, it has not been brought into thin film up to

now. Based on the attractive properties of chalcogenide thin films, such as earth abundance, environmentally friendly, potential in various applications, such as solar cells, ultraviolet light emitters, laser devices, spin functional devices, gas sensors, transparent electronics, corrosion resistant coating, microelectronics, optics, magnetic, and acoustic wave devices [9], and lack of information about $TlInS_{2-2x}Se_{2x}$ thin films, the present paper was prepared to pay attention to these films. In the present work, $Tl_2In_2S_3Se$ thin films were grown for the first time by physical deposition technique and its structural, morphological, and optical characteristics were investigated.

2 Experimental details

$Tl_2In_2S_3Se$ thin films were deposited on glass substrates using physical deposition technique. The powder of $Tl_2In_2S_3Se$ bulk crystals was compacted at around 500 MPa using a 15 tone capacity hydraulic press. The compacted sample was put in a tungsten boat and heated until the deposition rate of 1.0 Å/s becomes constant under the pressure of 150×10^{-6} Pa at room temperature using Nanovak NVTH-350 model thermal evaporator. Using an atmospheric control oven, the films were annealed at different temperatures for 30 min under nitrogen gas. Energy-dispersive spectroscopy (EDS) analysis were performed with a "JEOL JSM 6400" scanning electron microscope with tungsten source in ultra-high vacuum. For X-ray diffraction (XRD) experiments, Rigaku miniflex model diffractometer that emits CuK_α radiation at wavelength of 0.154049 nm from 10 to 90° with a speed of 0.02°/s was used. Shimadzu UV-1201 model spectrometer was used for optical transmission experiments in the 380–1000-nm region at room temperature. The surfaces of the films were analyzed by atomic force microscope (AFM), Veeco Nanoscope 5 in tapping mode. Raman scattering experiments were carried out by 532-nm Nd:YAG laser source using Horiba Jobin Yvon iHR550 imaging spectrometer, including triple grating monochromator. The thicknesses of the samples were measured about ~150 nm after deposition and annealing process using Dektak 6-M profilometer.

3 Results and discussion

3.1 Structural and morphological properties

Figure 1 shows the XRD patterns of the as-deposited and annealed $Tl_2In_2S_3Se$ thin films in the range of 10 to 60°. XRD pattern of the used source crystal for deposition was also presented in the figure. As seen from the figure, XRD pattern of the as-deposited thin film did not present any diffraction peak. This shows that the as-deposited thin films are in the amorphous form. One of the most important factors enabling the crystallization of amorphous thin films is annealing. In the compound, which is sent to the glass substrate by thermal evaporation, the atoms suddenly cool down before they can crystallize, and this causes the atoms to not sit in their required places in the crystal lattice. In the thin films exposed to the heat annealing process, the atoms migrate in the crystal lattice and crystallization takes place. With thermal annealing, dislocations, ductility, and hardness decrease. There are many examples in the literature on the temperature crystallization of amorphously grown thin films [10–12]. Taking into consideration this point, the deposited thin films were subjected to annealing process. As a result of the annealing processes carried out at different temperatures between 100 and 300 °C, it was understood that the thin films subjected to annealing temperature of 100 are also amorphous. Thin films annealed at 200 and 300 °C present diffraction peaks indicating that they exhibit crystallinity property. However, thin films annealed at 300 °C showed the high-quality crystallinity property. The XRD pattern of thin films annealed at 300 °C
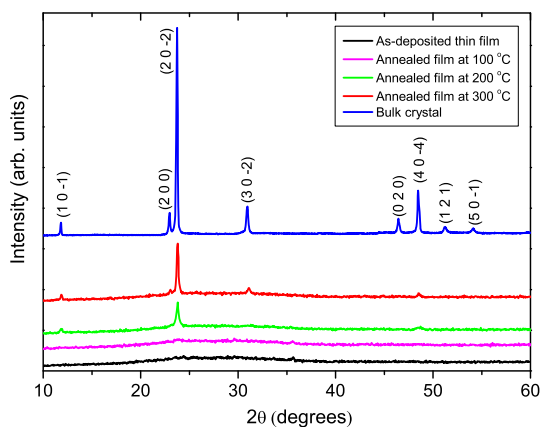

Fig. 1 XRD patterns of $Tl_2In_2S_3Se$ thin films and bulk crystal

showed a sharp peak around 23.80° and three weak peaks around 11.75°, 30.90°, and 48.50°. These diffraction peaks indicate that thin film has polycrystalline structure. The lattice parameters of the monoclinic unit cell calculated using a least-squares computer program DICVOL 04 were found to be $a = 0.8912$ nm, $b = 0.3981$ nm, $c = 0.8501$ nm, and $\beta = 119.49°$ in our previous work for bulk $Tl_2In_2S_3Se$ single crystal [13]. The observed peaks in the XRD patterns of annealed thin film are consistent with those observed for bulk crystal. The diffraction peaks observed in the XRD graph indicate that the annealed thin films have a quality crystalline structure [14].

$$D = \frac{0.9\lambda}{\beta \cos\theta}. \tag{1}$$

The crystallite size (D) of annealed thin film was found from the Scherrer's formula given in Eq. (1), where λ is the wavelength of the incident X-ray beam (Cu K$_\alpha$ = 1.54 Å), β is the full-width at half-maximum, and θ is the Bragg's diffraction angle [11].

The crystallite size of the annealed $Tl_2In_2S_3Se$ thin film was found from this expression using parameters of most intensive peak as 30.1 nm. From the crystallite size, the dislocation density ($\delta = 1/D^2$) of the film was determined as 1.10×10^{-3} lines nm^{-2}. Moreover the lattice strain ($\varepsilon = \beta\cos\theta/4\sin\theta$) of the film was calculated as 0.56. $Tl_2In_2S_3Se$ compound is formed as a result of the replacement of S-atoms with Se-atoms in the $TlInS_2$ compound. Therefore, comparing the values obtained for the $Tl_2In_2S_3Se$ material with the corresponding values of the $TlInS_2$ and $TlInSe_2$ compounds will give us valuable insights. In the literature, the crystalline size and dislocation density of the $TlInS_2$ thin film deposited by thermal evaporation technique and annealed at 423 K were reported as 34 nm and 0.87×10^{-3} lines nm^{-2} [15]. The crystalline size of TlInSe2 thin film having thickness of 195 nm and prepared by thermal evaporation technique was found as 56.4 nm [16].

EDS analysis was used to get information about atomic compositions of the annealed thin film. In Fig. 2, EDS spectrum of the $Tl_2In_2S_3Se$ thin film is presented. EDS analysis resulted in atomic compositional ratio of Tl:In:S:Se as 23.1:26.4:34.8:15.6. Considering the possible errors that may occur during the analysis, this atomic ratio is consistent with the chemical representation of $Tl_2In_2S_3Se$. Considering the XRD and EDS results, it was seen that the

annealed thin film had high-quality crystalline structure and the desired atomic proportion. Three-dimensional AFM surface morphology of the $Tl_2In_2S_3Se$ thin film is shown in the inset of Fig. 2 for the sample within the scan area of 5×5 μm. The root-mean-square roughness of the film was found as 0.54.

3.2 Optical properties

Raman spectroscopy and transmission techniques were used to examine the optical properties of the deposited $Tl_2In_2S_3Se$ thin film. Raman spectroscopy gives information about vibrational, electronic states, structural, and phonon properties of the materials. Raman spectra of the deposited thin film and source bulk crystal are represented in Fig. 3 in the $90-600$ cm^{-1} range. Raman spectrum of the single crystal presents vibrational modes around 133.2, 193.2, 204.1, 277.5, 288.6, and 340.7 cm^{-1}, while five modes around 130.6, 169.8, 277.2, 286.9, and 336.2 cm^{-1} were observed in the Raman spectrum of the thin-film structure. Raman modes in $TlInS_2$ and $TlInSe_2$ compounds were previously reported in Refs. [17, 18]. Taking into account the reported modes, observed peaks in the Raman spectrum of $Tl_2In_2S_3Se$ thin film may be associated with multiphonon absorption processes. As an example, the mode observed around 169 cm^{-1} may be associated with combination bands of $114 + 49$ cm^{-1} which were observed in Raman spectra of $TlInS_2$ and $TlInSe_2$.

The optical properties of the thin film were also examined by making transmission measurements at room temperature in the 380–1000-nm spectral range. The observed transmission spectrum is indicate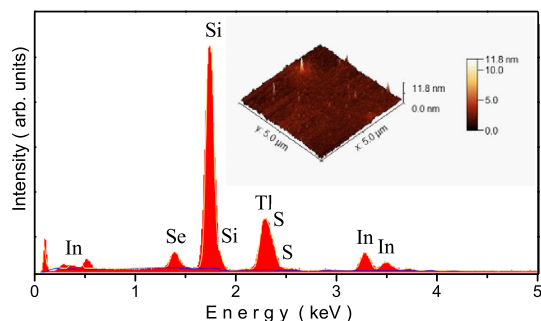d in Fig. 4. As can be seen from the figure, in the range of 400–650 nm, the film begins to partially absorb light, and the thin film completely absorbs the light below 400 nm. The band gap energy of the thin film was obtained by analyzing the transmission spectrum by two different methods: Derivative spectroscopy and Tauc analyses. In the derivative spectroscopy technique, the derivative of the transmission spectrum is taken with respect to the wavelength and $dT/d\lambda$ vs. λ graph is drawn. The peak maximum position(s) of the peak(s) observed in this plot corresponds to band gap energy [19]. The $dT/d\lambda$ vs. λ graph of the $Tl_2In_2S_3Se$ thin film is shown in the inset of Fig. 4. The graph drawn showed two peaks around 493 and 557 nm which correspond to energies of 2.52 and 2.23 eV. Considering the previously reported band gap energies of $Tl_2In_2S_3Se$, 2.23 and 2.52 eV were related to indirect and direct band gap energies. The analyses of transmission and reflection spectra of the $Tl_2In_2S_3Se$ single crystal presented the indirect and direct band gap energies as 2.16 and 2.42 eV, respectively [3]. When the band gap energies of the single crystal and the thin film were compared, it is seen that the energies of the thin film are slightly bigger. This is a result of the change of the band gap energy with thickness. It is known that as the thickness decreases, the band gap energy increases due to quantum confinement effect [20, 21]. In a recent paper, indirect and direct band gap energies of $TlInSe_2$ thin film were reported as 1.61 and 1.89 eV, respectively [16]. It is seen that replacement of S atom with Se results in decrease of band gap energy. This band gap energy tuning characteristics of the $TlInS_{2-2x}Se_{2x}$ provides a remarkable advantage for especially optoelectronic applications.

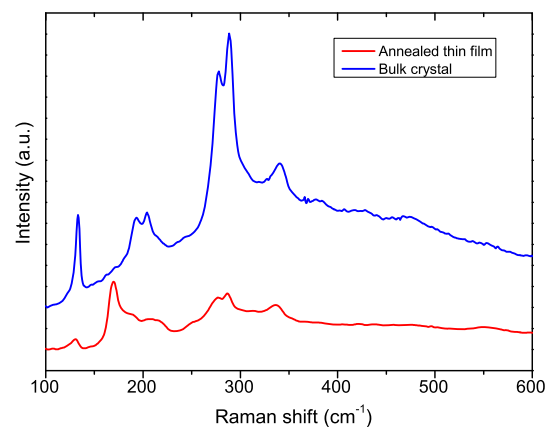**Fig. 2** EDS spectrum of annealed $Tl_2In_2S_3Se$ thin film. Inset indicates the AFM image of the film

Fig. 3 Raman spectra of $Tl_2In_2S_3Se$ thin film and bulk crystal
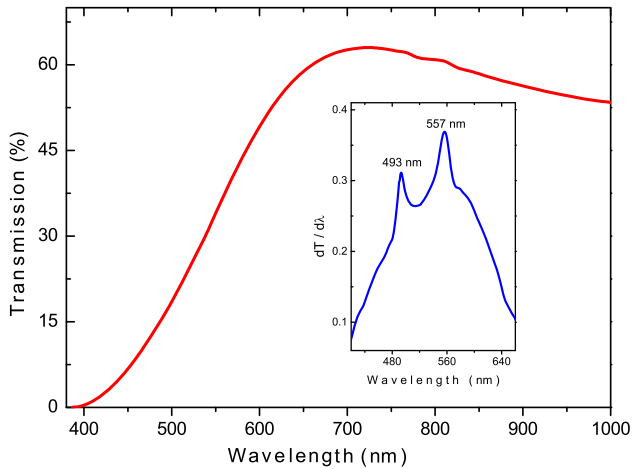
Fig. 4 Transmission spectrum of $Tl_2In_2S_3Se$ thin film. Inset indicates the $dT/d\lambda$ spectrum

Fig. 5 $(\alpha h v)^2$ vs. $h v$ plot for Tauc analysis. Solid line indicates the linear fitted line

Fig. 6 Photon energy-dependent absorption coefficient. Inset shows the $\ln(\alpha)$ vs. $h v$ plot for Urbach energy analysis

A second method of obtaining band gap energy is to use the Tauc equation which relates the band gap energy to absorption coefficient (α) as [22]

$$(\alpha h v) = A(h v - E_g)^p. \qquad (2)$$

The absorption coefficient is calculated from transmittance (T) and thickness (d) of the sample by $\alpha = (1/d) \ln (1/T)$. In Eq. (2), h is the Planck constant, v is the frequency, A is a parameter related with transition probability, and the p is 2 for indirect transition and 1/2 for direct transition. The band gap energy of the thin film can be found by plotting $(\alpha h v)^{1/p}$ vs. $h v$ graph. Figure 5 indicates the $(\alpha h v)^2$ vs. $h v$ plot which present linear dependency around the strong absorption region. The direct band gap energy of the $Tl_2In_2S_3Se$ thin film was found from the linear fit of the dependency as 2.52 eV which is well consistent with energy revealed from derivative spectral analyses method.

The dependency of absorption coefficient on photon energy represented in Fig. 6 can be used to get Urbach energy (E_u). The relation between α and E_u is given as follows [23]:

$$\alpha(h v) = \alpha_0 \exp(h v/E_u). \qquad (3)$$

When Eq. (3) is rearranged, it is seen that $\ln(\alpha)$ vs. $h v$ plot exhibits a linear behavior having slope of $1/E_u$. Inset of Fig. 6 shows the corresponding plot and applied linear fit. The Urbach energy was obtained from the slope as 0.58 eV.
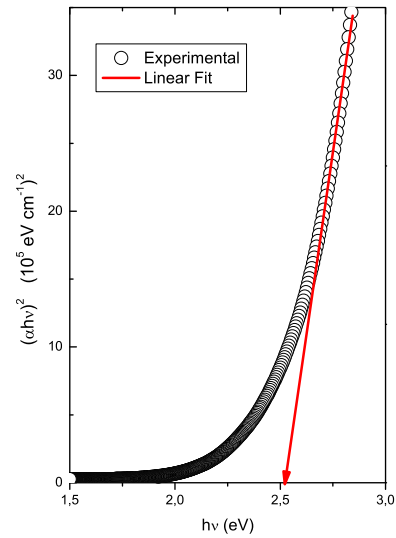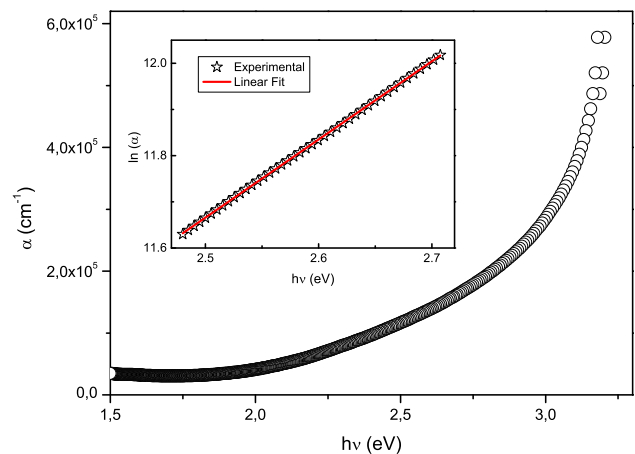
4 Conclusion

In this study, the structural, morphological, and optical properties of $Tl_2In_2S_3Se$ thin-film growth were examined. XRD pattern of the as-deposited thin film indicated that deposited thin films are in amorphous form. However, XRD pattern of the thin films annealed at 300 °C presented diffraction peaks. Most intensive peak observed around 23.80° was associated with (2 0–2) plane of the monoclinic crystal structure. EDS analyses showed that the atomic compositional ratio of the constituent elements in the thin film is consistent with chemical formula of $Tl_2In_2S_3Se$. Five vibrational modes around 130.6, 169.8,

277.2, 286.9, and 336.2 cm^{-1} were observed in the Raman spectrum of the thin film. Analyses of room-temperature transmittance spectrum showed that $Tl_2In_2S_3Se$ thin film has indirect and direct band gap energies of 2.23 and 2.52 eV, respectively. Urbach energy was determined from the photon energy-dependent absorption coefficient as 0.58 eV. $Tl_2In_2S_3Se$ compound belongs to layered structured semiconductors and have significant potential for 2D material technology. The present paper reports characteristics of $Tl_2In_2S_3Se$ thin film for the first time. The results presented in this paper would give a prediction about the 2D properties of $Tl_2In_2S_3Se$ material.

Author contributions

IG, MI, and NG contributed equally as a team, where all of them put their best effort to manage this work.

Data availability

The data that support the findings of this study are available from the corresponding authors upon reasonable request.

Declarations

Conflict of interest The authors have no competing interests to declare that are relevant to the content of this article.

References

1. M.M. El-Nahass, M.M. Sallam, A.H.S. Abd Al-Wahab, Optical and photoelectric properties of TlInS$_2$ layered single crystals. Curr. Appl. Phys. **9**, 311–316 (2009). https://doi.org/10.1016/j.cap.2008.02.011

2. M. Isik, N.M. Gasanly, Type="Italic">Effect of thallium (Tl) substitution for indium (In) on ellipsometric characteristics of TlInSe2 single crystals (Sci. Semicon. Proc, Mater, 2021). https://doi.org/10.1016/j.mssp.2021.106005

3. N.M. Gasanly, I. Guler, K. Goksen, Specific features of the optical spectra in Tl$_2$In$_2$S$_3$Se layered single crystals. Cryst. Res. Technol. **42**, 621–625 (2007). https://doi.org/10.1002/crat.200610874

4. T. Babuka, O.O. Gomonnai, K.E. Glukhov, L.Y. Kharkhalis, A.V. Gomonnai, M. Makowska-Janusik, Theoretical and experimental studies of electronic and optical properties of layered TlIn(S$_{0.75}$Se$_{0.25}$)$_2$ ferroelectric crystal. Integr. Ferroelectr. **220**, 18–29 (2021). https://doi.org/10.1080/10584587.2021.1921531

5. MYu. Tashmetov, F.K. Khallokov, N.B. Ismatov, I.I. Yuldashova, kh Umarov, Electronic irradiation of TlInS$_x$Se$_{2-x}$ ($x = 1$): morphology, structure and raman scattering. Int. J. Mod. Phys. B **35**, 2150289 (2021). https://doi.org/10.1142/S0217979221502891

6. I. Guler, N.M. Gasanly, Determination of trapping parameters of Tl$_2$In$_2$S$_3$Se layered single crystal by thermoluminescence. Cryst. Res. Technol. **53**, 1700134 (2018). https://doi.org/10.1002/crat.201700134

7. I. Guler, Optical analysis of TlInS$_{2x}$Se$_{2(1-x)}$ mixed crystals. J. Appl. Phys. **115**, 033517 (2014). https://doi.org/10.1063/1.4861640

8. I. Guler, N.M. Gasanly, Determination of trapping center parameters in Tl$_2$In$_2$S$_3$Se layered single crystals by thermally stimulated current measurements. Phys. B **404**, 2034–2038 (2009). https://doi.org/10.1016/j.physb.2009.03.035

9. H. Soonmin, I. Paulraj, M. Kumar, R.K. Sonker, P. Nandi, Recent developments on the properties of chalcogenide thin films, in *Chalcogenides - Preparation and Applications*. ed. by D. Vikraman (IntechOpen, UK, 2022)

10. R.M. Hassan, A.Z. Mahmoud, M.A. Abdel-Rahim, H.S. Assaedi, S.W. Alraddadi, A.M. Abd-Elnaiem, Effect of thermal annealing on structure and optical properties of amorphous As$_{30}$Te$_{64}$Ga$_6$ thin films. J. Inorg. Organomet. Polym. Mater. **31**, 3037–3053 (2021). https://doi.org/10.1007/s10904-021-01897-3

11. S. Mehraj, M.S. Ansari, Alimuddin, Annealed SnO_2 thin films: Structural, electrical and their magnetic properties. Thin Solid Films **589**, 57–65 (2015). https://doi.org/10.1016/j.tsf.2015.04.065

12. D. Negi, R. Shyam, S.R. Nelamarri, Role of annealing temperature on structural and optical properties of $MgTiO_3$ thin films. Mater. Lett. X **11**, 100088 (2021). https://doi.org/10.1016/j.mlblux.2021.100088

13. N.M. Gasanly, I. Guler, K. Goksen, Specific features of the optical spectra in $Tl_2In_2S_3Se$ layered single crystals. Cryst. Res. Technol. **42**, 621–625 (2007). https://doi.org/10.1002/crat.200610874

14. T. Buhari, D.K. Aktas, M. Erdem, G. Eryurek, The effect of crosslinker contents on the up-conversion luminescence properties of $CdNb_2O_6$: Er^{3+} powders embedded in the polyethylmethacrylate (PEMA) networks. J. Lumin. **251**, 119189 (2022). https://doi.org/10.1016/j.jlumin.2022.119189

15. M.M. El-Nahass, H.M. Zeyada, N.A. El-Ghamaz, A.E. Shetiwy, Particle size reduction of thallium indium disulphide nanostructured thin films due to post annealing. Optik **171**, 580–588 (2018). https://doi.org/10.1016/j.ijleo.2018.06.095

16. S.A. Al-Ghamdi, A.A.A. Darwish, T.A. Hamdalla, A.O.M. Alzahrani, S. Khasim, S.I. Qashou, Abd El-Rahman, Preparation of $TlInSe_2$ thin films using substrate temperature: characterization, optical and electrical properties. Opt. Mater. **129**, 112514 (2022). https://doi.org/10.1016/j.optmat.2022.112514

17. R. Paucar, Y. Shim, K. Wakita, O. Alekperov, N. Mamedov, Temperature dependence of low-frequency optical phonons in $TlInS_2$. Phys. Stat. Sol C **12**, 826–829 (2015). https://doi.org/10.1002/pssc.201400350

18. N. Kalkan, S. Celik, H. Bas, A.E. Ozel, Conduction mechanisms, molecular modelling and micro-raman studies of $TlInSe_2$ chalcogenide crystal. J. Optoelectron. Adv. M **19**, 234–245 (2017)

19. M. Isik, N.M. Gasanly, N.H. Darvishov, V.E. Bagiev, Effect of temperature on band gap of PbWO 4 single crystals grown by Czochralski method. Phys. Scr. **97**, 045803 (2022). https://doi.org/10.1088/1402-4896/ac576e

20. R.K. Kalaiezhily, V. Jayaseelan, K.K. Bharathi, M. Navaneethan, S.K. Eswaran, Thickness-dependent structural, optical, and dielectric properties of pulsed laser deposited Nb-doped $SrTiO_3$ thin films. J. Mater. Sci. Mater. El **33**, 8995–9002 (2022). https://doi.org/10.1007/s10854-021-07038-3

21. R.P. Khatri, A.J. Patel, Thickness dependent studies of chemically grown transparent conducting Cu:ZnS thin films for optoelectronic applications. Opt. Mater. **120**, 111469 (2021). https://doi.org/10.1016/j.optmat.2021.111469

22. R.H. Bube, *Photoelectronic Properties of Semiconductors* (Cambridge University Press, Cambridge, 1992)

23. M. Nagaraja, P. Raghu, H.M. Mahesh, J. Pattar, Structural, optical and Urbach energy properties of ITO/CdS and ITO/ZnO/CdS bi-layer thin films. J. Mater. Sci. Mater. El **32**, 8976–8982 (2021). https://doi.org/10.1007/s10854-021-05568-4